Direct Sagittal CT in the Evaluation of Temporal Bone Disease

Mahmood F. Mafee, Arvind Kumar, Christina N. Tahmoressi, Barry C. Levin, Charles F. James, Robert Kriz and Vlastimil Capek

AJNR Am J Neuroradiol 1988, 9 (2) 371-378
http://www.ajnr.org/content/9/2/371

Direct Sagittal CT in the Evaluation of Temporal Bone Disease

Mahmood F. Mafee[1]
Arvind Kumar[2]
Christina N. Tahmoressi[1]
Barry C. Levin[2]
Charles F. James[1]
Robert Kriz[1]
Vlastimil Capek[1]

The human temporal bone is an extremely complex structure. Direct axial and coronal CT sections are quite satisfactory for imaging the anatomy of the temporal bone; however, many relationships of the normal and pathologic anatomic detail of the temporal bone are better seen with direct sagittal CT sections. The sagittal projection is of interest to surgeons, as it has the advantage of following the plane of surgical approach. This article describes the advantages of using direct sagittal sections for studying various diseases of the temporal bone. The CT sections were obtained with the aid of a new headholder added to our GE CT 9800 scanner.

The direct sagittal projection was found to be extremely useful for evaluating diseases involving the vertical segment of the facial nerve canal, vestibular aqueduct, tegmen tympani, sigmoid sinus plate, sinodural angle, carotid canal, jugular fossa, external auditory canal, middle ear cavity, infra- and supralabyrinthine air cells, and temporomandibular joint.

CT has contributed greatly to an understanding of the complex anatomy and spatial relationship of the minute structures of the hearing and balance organs, which are packed into a small pyramid-shaped petrous temporal bone [1, 2]. In the past 6 years, high-resolution CT scanning has been rapidly replacing standard tomography and has proved to be the diagnostic imaging method of choice for studying the normal and pathologic details of the temporal bone [3–14]. CT of the temporal bone should always include at least two projections [5, 13, 15, 16]. The use of a single projection may lead to serious mistakes, since structures parallel to the plane of section are seen only partially or not at all [13]. The basic projection is of course the direct axial (horizontal) plane, since this is the most suitable and practical as well as the easiest projection to obtain for the baseline study of the temporal bone [5, 13]. Direct coronal sections can be obtained with many scanners; however, direct sagittal sections are hard or impossible to obtain because of the limitations of the CT scanners. The purpose of our study was to review the potential of direct sagittal CT (obtained with a new head-holder attached to our GE 9800 CT scanner) [17] in the diagnostic investigation of the diseases of the temporal bone and to demonstrate the important role of the sagittal projection in revealing certain anatomic and pathologic details of the temporal bone.

Materials and Methods

Although direct sagittal CT scans have been obtained in over 200 patients, our retrospective review encompassed a 2-year period during which 22 patients had surgical or clinical confirmation of CT findings that were seen best on direct sagittal CT scans (Table 1). The sagittal plane was scanned along with the axial or coronal plane. The direct sagittal plane was recommended on the basis of clinical histories and CT findings in the axial or coronal plane. Reasons for direct sagittal CT included the need for evaluating the vertical portion of the facial nerve canal, vestibular aqueduct, tegmen tympani, sigmoid sinus plate, external auditory canal, and temporomandibular joint.

This article appears in the March/April 1988 issue of *AJNR* and the June 1988 issue of *AJR*.

Received February 20, 1986; accepted after revision August 19, 1987.

Presented at the annual meeting of the American Society of Neuroradiology, San Diego, January 1986.

This work was supported in part by General Electric clinical application grant CT 2–5–37364.

[1] Department of Radiology, University of Illinois College of Medicine, and the University of Illinois Eye and Ear Infirmary, 1855 W. Taylor St., Chicago, IL 60612. Address reprint requests to M. F. Mafee.

[2] Department of Otolaryngology–Head and Neck Surgery, University of Illinois College of Medicine, and the University of Illinois Eye and Ear Infirmary, Chicago, IL 60612

***AJR* 9:371–378, March/April 1988**
0361–803X/88/0902–0371

TABLE 1: Findings in Patients with Disease of the Ear or Temporomandibular Joint Who Were Studied with Direct Sagittal CT

Case No.	Age	Gender	Clinical Diagnosis	CT Diagnosis	Final Diagnosis	Comments
1	34	M	Tender right mastoid	Aggressive infection vs neoplasm	Aggressive fibromatosis	Erosion of FNC and sigmoid plate best seen on sagittal scans
2	70	M	Hearing loss, middle ear mass	Mass in round window niche	Cochlear schwannoma	Location of tumor best seen on sagittal scans
3	34	F	Bulging red mass in right external ear canal; R/O glomus	Epidermoid cyst vs glomus	Cholesterol granuloma	Extent and location of cyst best seen on sagittal scans
4	13	M	S/P mastoidectomy, AS: R/O RC	Brain herniation and RC in mastoid bowl	Brain herniation and scar tissue	Tegmental defect best seen on sagittal scans
5	56	F	S/P mastoid surgery, AU: blue mass, AD	RC vs cholesterol granuloma, AD	Cholesterol granuloma, AD	Lesion best seen on sagittal scans
6	69	F	Mastoid surgery, AU	RC and encapsulated cyst, AS	Cholesterol granuloma	Bulging cyst best seen on sagittal scans
7	14	F	Sensorineural hearing loss, AD; R/O inner ear anomaly	Large vestibular aqueduct, AD	Large vestibular aqueduct	Sagittal view is view of choice for vestibular aqueduct
8	21	F	Profound hearing loss AS; R/O inner ear anomaly	Large vestibular aqueduct, AS	Large vestibular aqueduct	Sagittal view is view of choice for vestibular aqueduct
9	7	F	Hearing loss, AU; R/O congenital ear anomaly	Large vestibular aqueduct, AS	Large vestibular aqueduct	Sagittal view is view of choice for vestibular aqueduct
10	5	M	Facial deformity; hearing loss, AU	Deformity of ossicles, AU; large vestibular aqueduct, AU	No surgery planned	Large aqueduct best seen on sagittal scans
11	20	M	Car accident; CHL, facial paralysis, R/O Fx	Ossicular dislocation; Fx, left temporal bone; Fx, FNC	Fx, FNC; ossicular dislocation	Fx of FNC best seen on sagittal scans
12	26	M	Facial nerve paralysis, CHL, AS; Hx of trauma	Fx, dislocated ossicles, AS; Fx, FNC & tegmen	Fx, dislocation, AS	Fx of tegmen and FNC best seen on sagittal scans
13	40	M	Head trauma: CHL; R/O, Fx, ossicular, dislocation	Fx, dislocated ossicles	Fx, dislocated ossicles	Dislocation best seen on axial and sagittal scans
14	45	F	Tumor of EAC	Tumor of EAC	Squamous carcinoma of EAC	Extent of tumor best seen on axial and sagittal scans
15	27	F	Dislocation of right and left TMJ disks	Dislocation, both TMJ disks	Dislocation of both TMJ disks confirmed at surgery	Sagittal view is view of choice for TMJ
16	29	F	Dislocation of right TMJ disk	Dislocation	Dislocation confirmed at surgery	Sagittal view is view of choice for TMJ
17	11	M	Vascular mass, AU	High jugular bulb, AU	Dehiscent bone of hypotympanic floor; protruding jugular bulb, AU	Sagittal view is important view for jugular fossa
18	11	M	COM, polyp, AS	COM, AU; cholesteatoma, AS	COM, AU; cholesteatoma, AS	Erosion of ATS best seen on sagittal scans
19	42	M	Cholesteatoma, AS; facial paresis	Cholesteatoma, AS; normal FNC	Cholesteatoma, AS	Normal FNC; facial paresis resolved
20	10	F	Cholesteatoma, AS	Large cholesteatoma, AS, with defect of tegmen	Cholesteatoma, AS; tegmental defect	Tegmental defect best seen on sagittal scans
21	40	F	COM, AU; maximum hearing loss, AU; R/O tympanosclerosis	Cholesteatoma, AU; fistula, LSC, AD; erosion of sigmoid plate, AD	Cholesteatoma, fisula, LSC, AD; surgery planned for AS	CT enabled definitive Dx; extent of lesion best seen on sagittal scans
22	55	F	CHL, AD; R/O tympanosclerosis	Attic cholesteatoma	Intratympanic meningioma	Ectopic intratympanic meningioma

Note.—FNC = facial nerve canal; R/O = rule out; S/P = status post; AS = left ear; RC = recurrent cholesteatoma; AU = both ears; AD = right ear; CHL = conductive hearing loss; Fx = fracture; Hx = history; EAC = external auditory canal; TMJ = temporomandibular joint; COM = chronic otomastoiditis; ATS = anterior tympanic spine; LSC = lateral semicircular canal; Dx = diagnosis.

The group comprised 10 men and 12 women 5–70 years old. The CT scans were obtained on a GE CT/T 9800 unit by using 1.5-mm collimation with 0.25-mm^2 pixels and extended gray scales to 4000 H (+3,000–1,000 H). The sections were obtained at 1.5-mm intervals. The technique and methodology of direct sagittal CT scanning has been described in another article [17]. Contrast infusion (meglumine diatrizoate, 2 ml/kg body weight for children and a total of 150 ml for adults) was used in those patients suspected of having tumor of the temporal bone or acute suppurative infection of the ear, including infected cholesteatoma. In these cases additional sections (10 mm) of the head were also obtained to rule out possible intracranial complications.

Results

The radiographic and clinical findings in our patients are presented in Table 1. The sagittal CT scans were extremely useful in demonstrating the destruction of the sigmoid plate and facial nerve canal in a patient with aggressive fibromatosis of the mastoid (Fig. 1) and in showing the extension of a labyrinthine schwannoma into the round window niche in another patient (Fig. 2). In one patient with cholesterol granuloma of the middle ear, CT revealed a mass in the external canal and middle ear (Fig. 3). The exact extent of the mass and erosion of the anterior wall of the middle ear was demonstrated best on sagittal scans (Fig. 3B).

Three patients (cases 4–6) had previous mastoidectomies. In case 4 a large tegmental defect with associated brain herniation was demonstrated on sagittal and coronal CT sections (Fig. 4). The anatomic relationships of the mastoid cavity, tegmental defect, brain herniation, and facial nerve canal were better appreciated on sagittal scans (Fig. 4). In cases 5 and 6, CT revealed a large bulging mass in the mastoid cavity (Fig. 5); the masses were interpreted as recurrent cholesteatomas or cholesterol granulomas. At surgery both patients had cholesterol granulomas. The sagittal scans were most useful to the surgeon in demonstrating the relationship of these masses to the tegmen and sigmoid plate (Fig. 5B).

Four patients were suspected of having congenital ear anomalies (cases 7–10). Three of these (cases 7–9) had a large vestibular aqueduct, which was seen best on sagittal

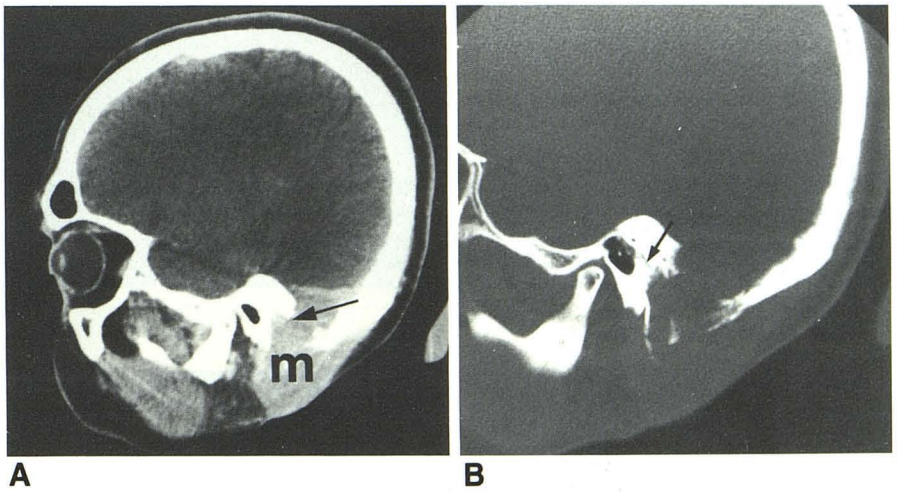

Fig. 1.—Case 1: aggressive fibromatosis of right mastoid region.

***A*, Direct sagittal CT scan shows destructive enhancing mass (m) eroding sigmoid plate (*arrow*) and nearly entire mastoid bone.**

***B*, Direct sagittal CT scan shows proximal portion of mastoid segment of facial nerve canal (*arrow*) and complete destruction of its distal portion. At surgery, facial nerve was surrounded by lesion. Despite extensive facial nerve involvement, the patient did not have facial paralysis.**

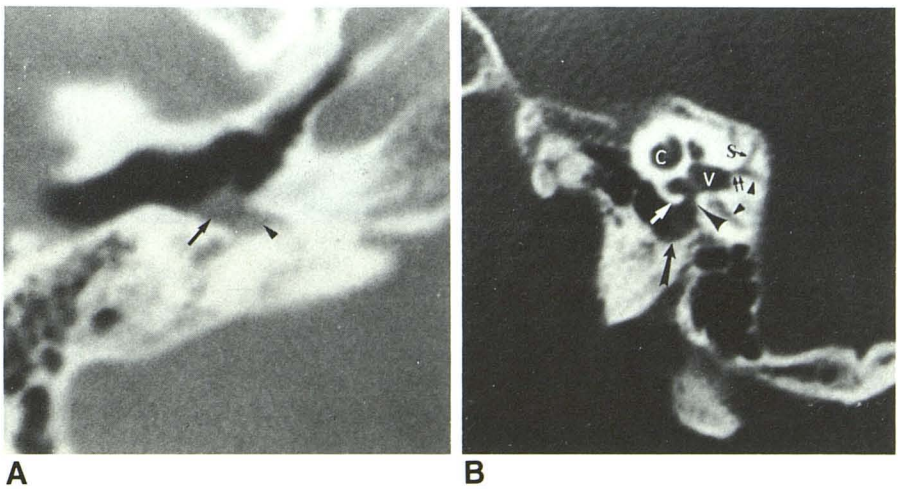

Fig. 2.—Case 2: cochlear schwannoma.

***A*, Axial CT scan shows soft-tissue mass (*arrow*) in middle ear, filling round window niche (*arrowhead*).**

***B*, Direct sagittal CT scan shows soft-tissue mass (*long black arrow*) filling round window niche. Slight widening of round window membrane (*large arrowhead*) is a clue that tumor is coming from scala tympani of cochlea into round window niche of middle ear cavity. Note promontory (*white arrow*), cochlea (c), vestibule (v), common crus (*short black arrows*), and superior (s) and posterior (*small arrowheads*) semicircular canals. At surgery this histologically proved schwannoma was found to have arisen from the cochlea and to extend through round window membrane into round window niche.**

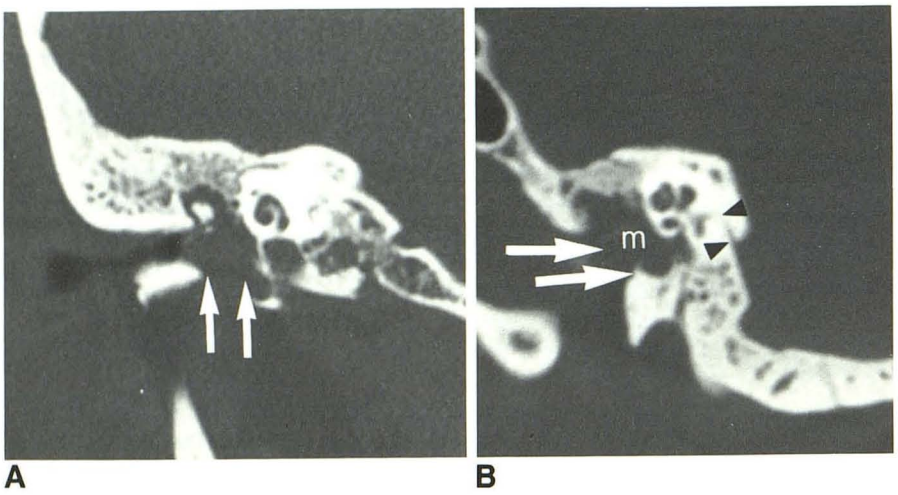

Fig. 3.—Case 3: cholesterol granuloma (cyst) of right ear.

A, Coronal CT scan of right temporal bone shows soft-tissue mass in middle ear and external auditory canal (*arrows*). Note erosion of floor of middle ear and external canal.

B, Direct sagittal CT scan shows soft-tissue mass (m) in right middle ear cavity, eroding anterior wall of middle ear (*arrows*) in region of carotid canal. Anatomic relationships of this mass are better appreciated in sagittal plane. Note normal vestibular aqueduct (*arrowheads*).

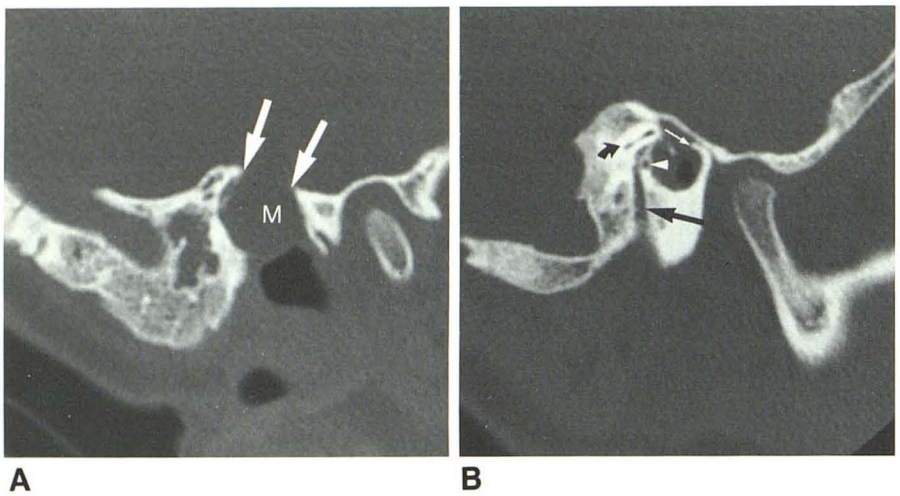

Fig. 4.—Case 4: recurrent cholesteatoma and brain herniation into mastoid cavity.

A, Direct sagittal CT scan shows large tegmental defect (*arrows*) with soft-tissue mass (M) bulging into mastoid bowl in patient with previous mastoidectomy.

B, Direct sagittal CT scan shows soft tissue in attic and middle ear. Vertical segment of facial nerve canal (*straight black arrow*) and lateral semicircular canal (*curved arrow*) are well outlined. Note density of stapedial muscle (*arrowhead*) and anterior tympanic spine (*white arrow*).

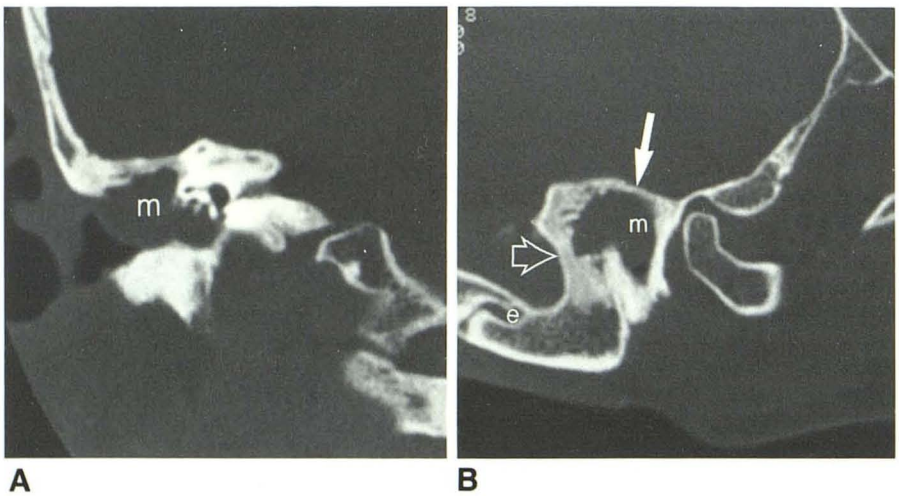

Fig. 5.—Case 5: cholesterol granuloma cyst.

A, Coronal CT scan shows postsurgical appearance of mastoidectomy, with large bulging soft-tissue mass (m) in right mastoid bowl protruding into external canal.

B, Direct sagittal CT scan shows soft-tissue mass (m) filling entire mastoid bowl and protruding into external canal. Relationship of mass to tegmen tympani (solid *arrow*) and sigmoid sinus plate (*open arrow*) is best evaluated on sagittal scan. Note mastoid emissary canal (e).

CT scans (Fig. 6). One patient (case 10) had an anomaly of the ossicles and large vestibular aqueduct in both ears.

In three patients with a history of trauma (cases 11–13), CT revealed fractures of the temporal bone. Sagittal CT scans were extremely helpful in evaluating the exact site of the fractures of the facial nerve canal (Fig. 7) and tegmen tympani (Fig. 8). The ossicular dislocation was best seen on sagittal and axial scans (Figs. 8A and 9). The sagittal plane was most

Fig. 6.—Case 7: large vestibular aqueduct. Direct sagittal CT scan shows marked enlargement of vestibular aqueduct (*arrows*). (Compare with normal vestibular aqueduct in Fig. 3B.)

Fig. 7.—Case 11: comminuted fracture of temporal bone with involvement of facial nerve canal. Direct sagittal CT scan shows linear fracture of mastoid (*solid black arrow*), which extends to and involves vertical segment of facial nerve canal (*arrowhead*). Bone fragment (*open arrow*) compressing facial nerve was confirmed at surgery. Note fracture of sigmoid plate (*curved arrow*) and fractures of retrofacial air cells. Increased soft tissue (S) in anterior tympanic cavity is from involvement of supratubal air cells and canal for tensor tympani. Clouding of supratubal and retrofacial air cells is from intraluminal and submucosal bleeding. Findings were confirmed at surgery.

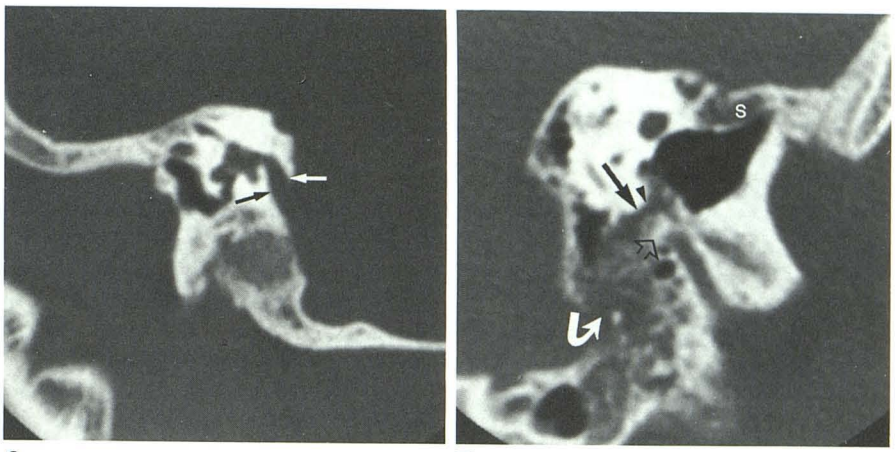

6 7

Fig. 8.—Case 12: fracture of temporal bone with ossicular dislocation.

A, Direct sagittal CT scan shows fracture of anterior wall of external canal (*black arrow*) and posterosuperior dislocation of incus (*white arrow*).

B, Direct sagittal CT scan shows increased soft tissue in region of canal for tensor tympani with bone fragment (*solid arrow*). Note discontinuity of tegmen and fracture in region of geniculate ganglion (*open arrow*). Findings were confirmed at surgery.

A B

Fig. 9.—Case 13: incudomalleal dislocation. Direct sagittal CT scan shows separation of malleus (m) and incus (i). Note undisplaced fracture of anterior wall of middle ear cavity (*straight white arrow*), pyramidal eminence (*curved arrow*), facial nerve canal (*long black arrow*), and lateral, superior, and posterior semicircular canals (*short black arrows*).

Fig. 10.—Case 14: squamous cell carcinoma of external auditory canal. Direct sagittal CT scan shows soft-tissue tumor (m) with erosion of inferior and anterior walls of external auditory canal. Isolated bone fragment (*arrow*).

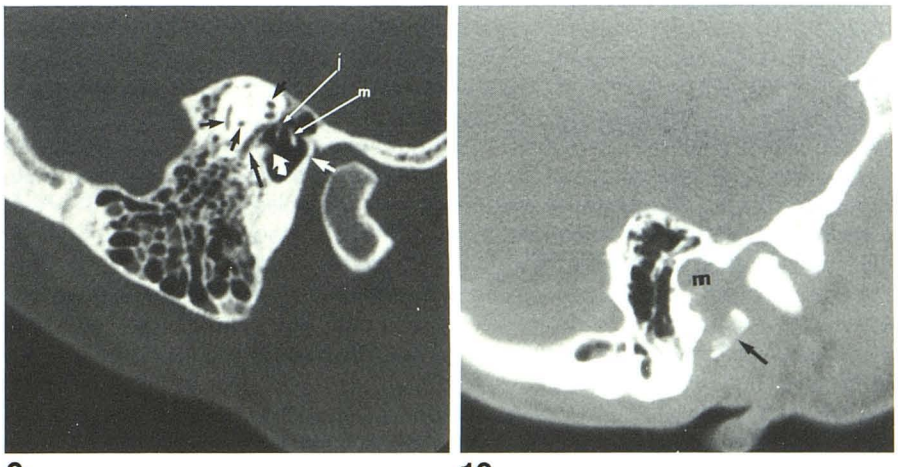

9 10

informative in demonstrating the tumor extent in a patient with squamous cell carcinoma of the external auditory canal (Fig. 10). Dislocation of the temporomandibular disk was demonstrated best on sagittal CT scans in cases 15 and 16 (Fig. 11). Protrusion of the jugular veins into the middle ear cavities from dehiscent jugular fossae and the relationship of jugular veins to the round window membranes were best evaluated on sagittal CT scans in a patient found to have a bluish mass behind both tympanic membranes (Fig. 12).

One patient (case 18) was diagnosed as having a small

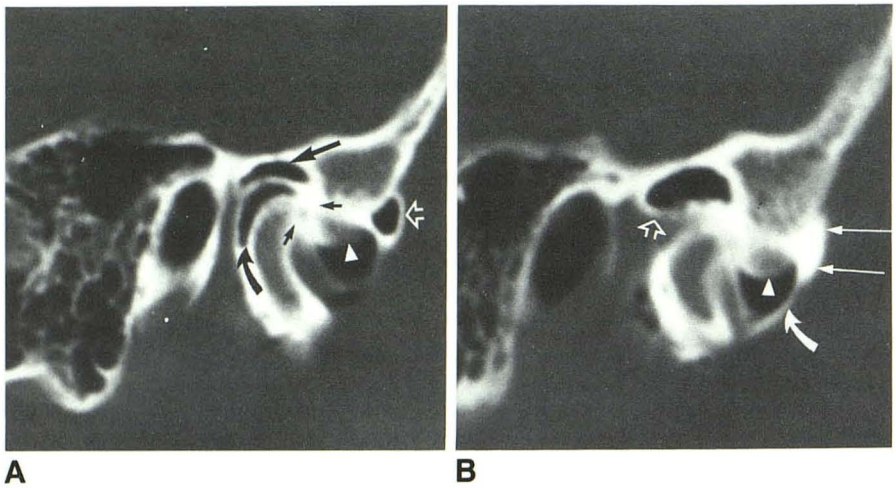

Fig. 11.—Case 15: anterior dislocation of left temporomandibular joint meniscus without reduction.

***A*, Direct sagittal CT air-positive contrast arthrogram in closed-mouth position shows dislocated left meniscus (*arrowhead*). Air is in superior joint space (*long straight black arrow*) and in inferior joint space (*curved arrow*), and air and contrast material are in anterior recess of superior joint space (*open arrow*). Contrast material is also seen just superior and inferior to displaced meniscus (*short straight black arrows*).**

***B*, Direct sagittal CT scan in open-mouth position clearly shows unreduced meniscus (*arrowhead*). In this position iodinated contrast material has replaced air in anterior recess of superior joint space (*solid straight arrows*). Note stretching of retrodiskal or bilaminar zone (*open arrow*). Joint capsule is outlined by air and positive contrast (*curved arrow*).**

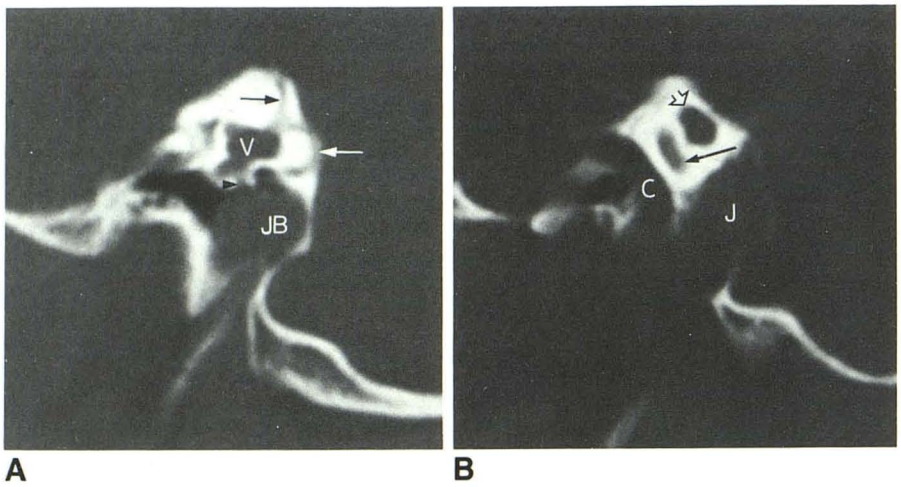

Fig. 12.—Case 17: high and dehiscent jugular fossa with protrusion of jugular bulb into tympanic cavity, simulating vascular mass.

***A*, Direct sagittal CT scan shows jugular bulb (JB). Bone defect is along floor of hypotympanum with jugular bulb bulging into middle ear up to level of round window membrane (*arrowhead*). Note vestibule (V) and superior (*black arrow*) and posterior (*white arrow*) semicircular canals.**

***B*, Direct sagittal CT scan 4.5 mm medial to *A* shows carotid canal (C), jugular fossa (J), basal turn of cochlea (*solid arrow*), and internal auditory canal (*open arrow*). Jugular fossa is quite high in position and reaches level of internal auditory canal.**

attic cholesteatoma after CT showed erosion of the anterior tympanic spine, which was seen best on sagittal scans. Erosion of the facial nerve canal was clinically suspected in a patient with a cholesteatoma in the left ear. In this patient (case 19), CT revealed a large atticoantral cholesteatoma eroding the retrofacial air cells and thinning out the posterior margin of the proximal portion of the mastoid segment of the facial nerve canal. The anatomic relationships of the cholesteatoma and facial nerve canal were delineated best on sagittal scans. At surgery, the CT findings were confirmed, with the cholesteatoma eroding the retrofacial air cells but not extending into the facial nerve canal. One patient with a cholesteatoma (case 20) had erosion of the tegmen tympani, which was seen best on sagittal CT scans.

Two patients were clinically diagnosed as having tympanosclerosis (cases 21 and 22). In case 21, bilateral cholesteatomas were found with erosion of the lateral semicircular canal and sigmoid sinus plate. The sigmoid sinus plate defect was depicted best on sagittal scans. In case 22 (the second patient with the clinical diagnosis of tympanosclerosis), CT revealed the classic findings of an attic cholesteatoma, with erosion of the lateral attic wall, anterior tympanic spine, and ossicles. To our surprise, an intratympanic (ectopic) meningioma was found at surgery. In this patient, postoperative contrast-enhanced CT, including thin axial, coronal, and sagittal sections (superior for jugular fossa and sublabyrinthine air cells) of the posterior fossa and base of the skull and temporal bone, did not show any mass in the posterior fossa or base of the skull.

Discussion

The radiographic anatomy of the complex structures of the human temporal bone has always been a challenge to radiologists. The introduction of tomography in the late 1930s as a technique for body-section imaging was an important step in the radiographic delineation of the minute structures of the ear [18]. However, a practical application for studying the temporal bone was not available until 20 years later, when multidirectional tomographic units became commercially available [18, 19]. Before the introduction of high-resolution CT, complex-motion tomography was the diagnostic imaging method of choice for studying the anatomy and morphologic

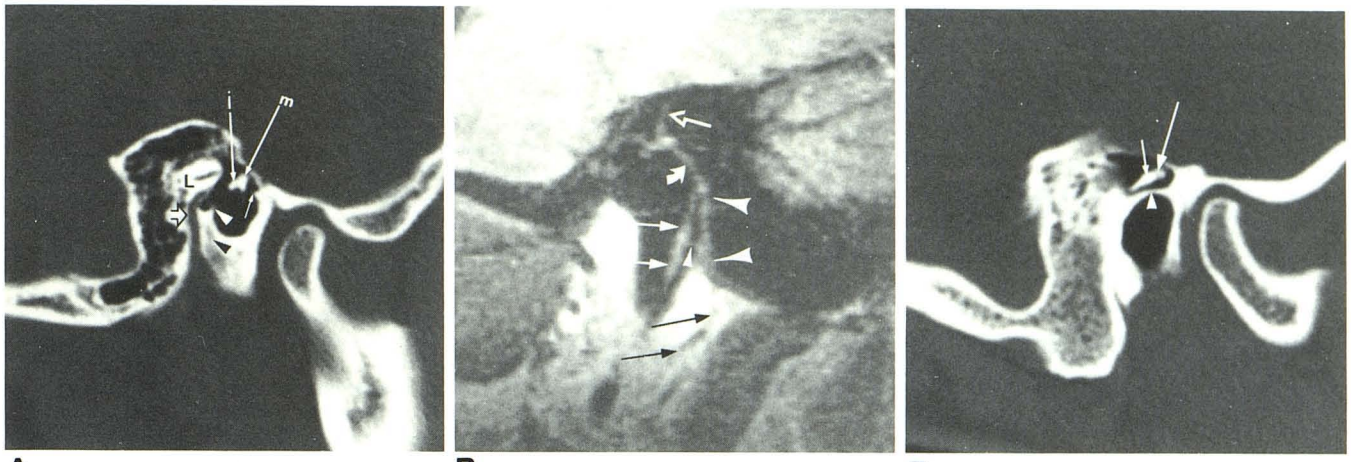

Fig. 13.—*A*, Normal facial nerve canal. Direct sagittal CT scan shows entire mastoid segment of facial nerve canal (*open arrow*). Immediately below lateral semicircular canal (L) is posterior portion of tympanic segment of facial nerve canal. Note incus (i), malleus (m), anterior tympanic spine (*white arrow*), pyramidal eminence (*white arrowhead*), and low density of stapedius canal (*black arrowhead*) in front of facial nerve canal. (Compare with *B*.)

***B*, Normal facial nerve. Sagittal partial-saturation T1-weighted MR scan (repetition time = 800 msec, echo time = 25 msec) obtained with surface receiver coil shows superior semicircular canal (*open arrow*), posterior portion of tympanic segment of facial nerve (*curved arrow*), mastoid (*large arrowheads*) and parotid (*black arrows*) segments of facial nerve. Note stapedius muscle (*straight white arrows*), which originates within pyramidal eminence in front of vertical (mastoid) portion of facial nerve. Small structure (*small arrowhead*) extending from facial nerve to stapedius muscle is believed to represent stapedius nerve.**

***C*, Normal ossicles. Direct sagittal CT scan shows malleus (*long arrow*), incus (*short arrow*), inferior aspect of lateral wall of attic (*arrowhead*), and temporomandibular joint.**

alteration of the bony structures of the temporal bone and base of the skull [18, 19].

In the past 6 years CT has rapidly been replacing complex-motion tomography and has proved to be the diagnostic imaging method of choice for assessing the temporal bone [1–14]. Three prerequisites are necessary for the study of the temporal bone: high definition, thin sections, and multiple projections [13]. Direct axial and coronal CT sections are quite satisfactory for demonstrating the anatomy of the temporal bone; however, study of the axial or coronal sections should be supplemented by direct sagittal sections. The sagittal projection is of much interest to surgeons as it has the advantage of following the plane of surgical approach [19]. Many relationships of the structure of the temporal bone are better seen by studying direct sagittal CT sections of the temporal bone. This projection is particularly satisfactory for studying the normal and pathologic details of the mastoid segment of the facial nerve canal (Figs. 7, 13A, and 13B), ossicles (Figs. 8A, 9, and 13C), vestibular aqueduct (Figs. 3 and 6), tegmen tympani (Figs. 4A and 8B), sigmoid plate (Figs. 1 and 7), external auditory canal (tympanic bone) (Fig. 10), mastoid (Fig. 1), jugular fossa (Fig. 12A), carotid canal (Fig. 12B), supra-sublabyrinthine air cells (Figs. 8B and 9), and retrofacial air cells (Figs. 7 and 13A). We recommend the direct sagittal projection to evaluate the vestibular aqueduct (Fig. 6); fractures of the temporal bone (Figs. 7–9); patients with infranuclear facial paralysis; and diseases involving the round window niche (Fig. 2), tegmen tympani (Fig. 4A), sigmoid sinus plate (Fig. 7), carotid canal (Fig. 12B), jugular fossa (Fig. 12), external auditory canal (Fig. 10), and temporomandibular joint (Fig. 11). In our institution the sagittal projection has proved extremely valuable for assessing the extent of

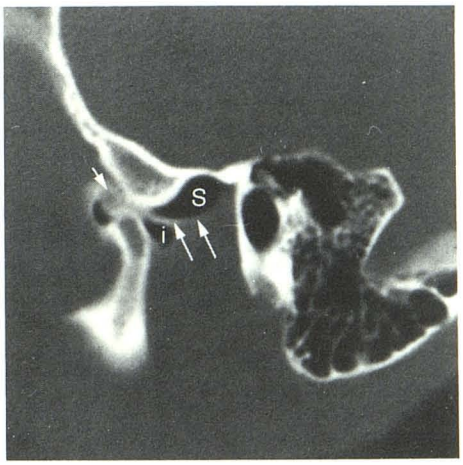

Fig. 14.—Case 15: dislocated right temporomandibular joint meniscus. Direct sagittal CT air-positive contrast arthrogram in open-mouth position shows dislocated disk (*short arrow*). Air is in superior (S) and inferior (i) joint spaces. Note stretching of retrodiskal zone (*long arrows*).

atticoantral cholesteatoma and its relationship to the sigmoid plate and tegmen tympani. This projection is essential for evaluation of the mastoid segment of the facial nerve canal (Figs. 1B and 7), vestibular aqueduct (Fig. 6), and temporomandibular joint (Fig. 11). In our institution, whenever a trans- or retrolabyrinthine surgical approach is planned, a preoperative sagittal CT scan of the temporal bone is obtained at the request of the surgeons so they can evaluate the relationship

of the jugular fossa to the internal auditory canal (Fig. 12B) and assess the relationship of the vertical segment of the facial nerve canal to the posterior wall of the external auditory (tympanic sulcus) canal and sigmoid sinus plate (Fig. 13A).

The sagittal plane in general is complementary to the coronal and axial planes, since it shows the anterior to posterior aspects of structures seen laterally to medially on coronal sections (Fig. 3) and the inferior to superior aspects of structures seen anteriorly to posteriorly on axial sections (Fig. 2) [15, 16, 18]. In our series, the direct sagittal projection proved to be extremely valuable in several cases (Table 1). Therefore, we believe this projection should be used to complement the axial and coronal planes, depending on the disease and the anatomic details to be imaged.

Disadvantages of the direct sagittal technique are the additional radiation, time, and effort. In many cases, the information obtained with axial and sagittal planes may be sufficient, obviating coronal sections. In temporal bone fractures, lesions of the external auditory canal, and diseases involving the vestibular aqueduct, round window niche, round window membrane, tegmen tympani, and sigmoid sinus plate, axial and sagittal CT scans are recommended.

Sagittal CT is essential for evaluating lesions of the temporomandibular joint (Fig. 10). The demarcation between disk and retrodiskal tissue (bilaminar zone) can be established easily on sagittal CT scans (Fig. 14). CT arthrography is an invasive method requiring technical skill and radiation exposure. In our institution, CT arthrography has proved to be a valuable and complementary diagnostic tool in the examination and treatment of patients with jaw dysfunction. The application of our sagittal head-holder is not limited to the temporal bone and temporomandibular joint. We have found it very useful for the evaluation of the other craniofacial structures, including sphenoethmoid complex, sella turcica, and the orbits (Fig. 1A).

ACKNOWLEDGMENTS

We thank Ruben Stortzum for technical expertise and assistance in manufacturing the sagittal head-holder and Mari Salazar for secretarial assistance.

REFERENCES

1. Shaffer KA, Haughton VW, Wilson CR. High resolution computed tomography of the temporal bone. *Radiology* **1980**;134:409–414
2. Valvassori GE, Mafee MF, Dobben GD. Computerized tomography of the temporal bone. In: *Proceedings of the Sixth Shambaugh International Workshop of Otomicrosurgery*. Huntsville, AL: Strode, **1980**:000–000
3. Valvassori GE, Mafee MF, Dobben GD. Computerized tomography of the temporal bone. *Laryngoscope* **1982**;92:562–565
4. Lufkin R, Barni JJ, Glen W, Mancuso A, Canalis R, Hanafee W. Comparison of computed tomography and pleuridirectional tomography of the temporal bone. *Radiology* **1982**;143:715–718
5. Mafee MF, Kumar A, Yannias D., Valvassori GE, Applebaum EL. Computed tomography of the middle ear in the evaluation of cholesteatomas and other soft tissue masses: comparison with pleuridirectional tomography. *Radiology* **1983**;148:465–472
6. Mafee MF, Valvassori GE, Dobben GD. The role of radiology in surgery of the ear and skull base. *Otolaryngol Clin North Am* **1982**;15:723–753
7. Mafee MF, Valvassori GE, Shugar MA, Yannias DA. High resolution and dynamic sequential computerized tomography in the evaluation of glomus complex tumors. *Arch Otolaryngol* **1983**;109:691–696
8. Swartz JD, Goodman RS, Russell KB, Marlowe FI, Wolfson RJ. High-resolution computed tomography of the middle ear and mastoid. Part II: Tubotympanic disease. *Radiology* **1983**;148:455–459
9. Mafee MK, Aimi K, Valvassori GE. Computed tomography in the diagnosis of primary tumors of the petrous bone. *Laryngoscope* **1984**;94:1423–1430
10. Mafee MF, Singleton EL, Valvassori GE, Espinosa GA, Kumar A, Aimi K. Acute otomastoiditis and its complications: role of CT. *Radiology* **1985**;155:391–397
11. Mafee MF, Henrickson GC, Deitch RL, et al. Use of CT in the stapedial otosclerosis. *Radiology* **1985**;156:709–714
12. Mafee MF, Valvassori GE, Deitch RL, et al. Use of CT in the evaluation of cochlear otosclerosis. *Radiology* **1985**;156:703–708
13. Valvassori GE, Mafee MF. The temporal bone. In: Carter BL, ed. *Computed tomography of the head and neck.* New York: Churchill Livingstone **1985**:171–205
14. Mafee MF, Aimi K, Kahen H, Capek V. Chronic otomastoiditis. A conceptual understanding of CT findings. *Radiology* **1986**;160:193–200
15. Zonneveld FW. The value of non-reconstructive multiplanar CT for the evaluation of the petrous bone. *Neuroradiology* **1983**;25:1–10
16. Zonneveld FW, Van Waes PFG, Damsma P, Rabischong P, Vignaud J. Direct multiplanar computed tomography of the petrous bone. *Radiographics* **1983**;3:410–449
17. Heffez L, Mafee MF, Langer B. Use of a new head holder for obtaining direct sagittal CT images of the TMJ. *J Oral Maxillofac Surg* **1987**;45:822–824
18. Valvassori GE, Buckingham RA. *Tomography and cross-sections of the ear.* Stuttgart: George Thieme, **1975**
19. Buckingham RA, Valvassori GE. Tomographic anatomy of the temporal bone. *Otolaryngol Clin North Am* **1973**;6:337–362